



저작자표시-비영리-변경금지 2.0 대한민국

이용자는 아래의 조건을 따르는 경우에 한하여 자유롭게

- 이 저작물을 복제, 배포, 전송, 전시, 공연 및 방송할 수 있습니다.

다음과 같은 조건을 따라야 합니다:



저작자표시. 귀하는 원저작자를 표시하여야 합니다.



비영리. 귀하는 이 저작물을 영리 목적으로 이용할 수 없습니다.



변경금지. 귀하는 이 저작물을 개작, 변형 또는 가공할 수 없습니다.

- 귀하는, 이 저작물의 재이용이나 배포의 경우, 이 저작물에 적용된 이용허락조건을 명확하게 나타내어야 합니다.
- 저작권자로부터 별도의 허가를 받으면 이러한 조건들은 적용되지 않습니다.

저작권법에 따른 이용자의 권리는 위의 내용에 의하여 영향을 받지 않습니다.

이것은 [이용허락규약\(Legal Code\)](#)을 이해하기 쉽게 요약한 것입니다.

[Disclaimer](#)

공학석사 학위논문

**Development of Solubilized Extracellular  
Matrix-Coated Composite Scaffolds to  
Facilitate Osteogenic Differentiation of  
Human Mesenchymal Stem Cell**

세포외기질이 코팅된 스캐폴드를 이용한  
인간 중간엽 줄기세포의 골분화 유도

2021년 2월

서울대학교 대학원

바이오엔지니어링전공

고 경 원

# Development of Solubilized Extracellular Matrix-Coated Composite Scaffolds to Facilitate Osteogenic Differentiation of Human Mesenchymal Stem Cell

지도교수 박 태 현

이 논문을 공학석사학위논문으로 제출함

2020년 12월

서울대학교 대학원

공과대학 협동과정 바이오엔지니어링 전공

고 경 원

고경원의 석사학위논문을 인준함

2020년 12월

위 원 장

김 병 수



부위원장

박 태 현



위 원

황 석 연



## ABSTRACT

# **Development of Solubilized Extracellular Matrix-Coated Composite Scaffolds to Facilitate Osteogenic Differentiation of Human Mesenchymal Stem Cell**

Kyungwon Ko

Interdisciplinary Program for Bioengineering

The graduate school

Seoul National University

Due to its heterogeneity of the extracellular matrix (ECM) microenvironment, various tissue engineering approaches have been used to recapitulate the mechanical and biochemical properties similar to its native ECM. Compared to other synthetic substrates imitating ECM, the decellularized extracellular matrix (dECM) is an excellent candidate for mimicking its native tissue microenvironment. Recently, dECM produced by cultured cells has emerged as efficient substrates facilitating cell expansion and differentiation, and solubilizing it into concentrated solutions could be a benefit for utilizing it in various substrates while still retaining ECM proteins promoting cellular functions. Since the composition of ECM proteins in solubilized dECM varies by which solubilizing reagents are used, an effective solubilization

method should be developed. In this study, MC3T3-E1-derived dECM was solubilized with collagenase (Cg-ECM), pepsin (P-ECM), urea (U-ECM), or guanidine-HCl (G-ECM). Each of the differently solubilized/digested dECM was compared to evaluate its osteogenic capacities by measuring ALP activities, ARS mineralization abilities, and expression levels of osteogenic marker genes of several dECM groups were assessed using real-time qPCR. Among differently solubilized ECM groups, G-ECM was effectively inducing osteogenic differentiation of hMSCs, and its effectiveness was further evaluated in the 3D scaffold. Hydroxyapatite embedded poly(lactide-co-glycolide) scaffold (PLGA/HA scaffold) coated with the polydopamine solution and solubilized G-ECM facilitated cell proliferation and osteogenic differentiation of hMSCs. Assuming its osteogenic capacities, dECM solubilized with Guanidine-HCl could replicate key features inducing osteogenic differentiation, and G-ECM coated scaffolds would be used as a new osteoinductive material for regenerative medicine and tissue engineering.

Keywords: cell-derived extracellular matrix, mesenchymal stem cell, osteogenesis, tissue engineering, regenerative medicine

Student number: 2019-26203

# Contents

<b>Abstract</b> .....	<b>i</b>
<b>Contents</b> .....	<b>iii</b>
<b>List of Figures and Table</b> .....	<b>v</b>
<b>1. Introduction</b> .....	<b>1</b>
<b>2. Materials and Methods</b> .....	<b>5</b>
2.1. Preparation of dECM .....	5
2.2. Solubilization of dECM .....	6
2.3. Coating of tissue culture plates with dECM .....	7
2.4. hMSCs culture and osteogenic differentiation .....	8
2.5. Cell proliferation assay .....	9
2.6. ALP and ARS staining .....	10
2.7. qRT-PCR on osteogenic marker gene .....	11
2.8. Fabrication of HA-coated paraffin spheres .....	12
2.9. Fabrication of PLGA/HA scaffolds .....	13
2.10. Polydopamine and G-ECM coating on the scaffold .....	14
2.11. Characterization of spheres and scaffolds .....	15
2.12. Statistical analysis .....	16
<b>3. Results and discussions</b> .....	<b>17</b>
3.1. Production of decellularized ECM and solubilized dECM .....	17
3.2. G-ECM coating induces cell proliferation and osteogenic differentiation of hMSCs .....	19
3.3. Fabrication and characterization of HA-coated paraffin spheres .....	24

3.4. Fabrication and characterization of the scaffolds .....	28
3.5. G-ECM composite scaffold promotes osteogenesis of hMSCs .....	32
<b>4. Conclusions .....</b>	<b>37</b>
<b>5. Reference .....</b>	<b>38</b>
국문초록 .....	41

## List of Figures and table

<b>Figure 1.</b> Schematic diagram of the research .....	4
<b>Figure 2.</b> Proliferation abilities of hMSCs cultured on solubilized dECM .....	20
<b>Figure 3.</b> ALP activities staining and quantification of hMSCs .....	21
<b>Figure 4.</b> ARS staining and quantification of hMSCs .....	22
<b>Figure 5.</b> Osteogenic marker gene expression levels of hMSCs .....	23
<b>Figure 6.</b> SEM images of paraffin and HA-coated paraffin spheres .....	25
<b>Figure 7.</b> EDS analysis of paraffin and HA-coated paraffin spheres .....	26
<b>Figure 8.</b> FTIR analysis of paraffin and HA-coated paraffin spheres .....	27
<b>Figure 9.</b> Optical and SEM images of scaffolds .....	29
<b>Figure 10.</b> EDS analysis of scaffolds .....	30
<b>Figure 11.</b> FTIR analysis of scaffolds .....	31
<b>Figure 12.</b> The proliferation abilities of hMSCs cultured on scaffolds .....	33
<b>Figure 13.</b> ALP activities quantification of hMSCs on scaffolds .....	34
<b>Figure 14.</b> ARS staining and quantification of hMSCs on scaffolds .....	35
<b>Figure 15.</b> Osteogenic marker gene expression levels of hMSCs on scaffolds .....	36
<b>Table 1.</b> The protein concentration of solubilized dECM .....	18

# 1. Introduction

Bone defects due to traumatic bone injury, inflammation, and other bone diseases are common in clinical practice, and autologous or allogeneic bone grafting is the most commonly applied method for healing bone defects. These conventional methods still have limitations, such as additional surgical invasion at a donor site, a limited quantity of grafts, and disease transmission [1, 2]. For these reasons, various bone regeneration approaches, including tissue engineering, biomaterials, and stem cells, have been studied. Biomaterial plays a vital role in providing structural support to the cells to facilitate cell growth and assist transportation of essential nutrients. Over the last decade, various scaffolds have been developed with synthetic materials using particulate leaching, phase separation, electrospinning, and 3D bioprinting technology, and they have been used extensively as artificial scaffolds for bone repair [3-8]. However, these synthetic polymer scaffolds often have insufficient osteoconductivity due to the lack of osteoinductive factors. Also, synthetic polymer alone could not fully mimic a tissue's microenvironment as they lack the innate capacity to actively modulate cell phenotype to form distinct tissue or organs [9].

Alternatives to these synthetic materials, the extracellular matrix (ECM) derived materials could be used as natural biomaterial additives for tissue engineering scaffolds. The ECM not only provides physical support for maintaining the structural integrity of tissues but also serves as a reservoir for biochemical and biophysical cues to support cell adhesion, proliferation, and differentiation [10]. Since tissue-specific functionalities are accompanied by dynamic remodeling of the ECM, cells of each tissue are responsive to the ECM in a process referred to as bidirectional crosstalk between the cell and its environment [11-13]. To utilize the ECM as biomaterials, ECM produced from tissue explants should be decellularized

removing cells and cellular components as these remnants might elicit immune responses [14]. The ECM produced from decellularization processes (dECM) still preserves structural proteins and other small molecules, improves cell growth and viability, and induces tissue repair and remodeling [15]. On top of that, cells cultured on dECM exhibit various desirable behaviors that cannot currently be replicated with synthetic or fully defined, artificial substrate. Therefore, dECM have been widely used in many applications in bone regeneration [16, 17].

However, these dECM produced from native tissues or organs are limited in supply, and they lack reproducibility and tailorability because of unwanted damage to ECM from harsh decellularization procedures. On the contrary, dECM produced from in vitro cell cultures offer several advantages over tissue-derived dECM. Cell-derived dECM could be produced in various structures, and they could be produced easily on a large scale. Besides, it is possible to modulate the properties of dECM by using different types of culturing substrates or co-culturing different types of cells. Although cell-derived dECM cannot fully reproduce the 3D microenvironment of native tissues, several studies suggested that cell-derived dECM have the potentials to regulate cellular behavior and functions [18-23].

While utilizing cell-derived dECM as cell culture substrates promotes cell adhesion, proliferation, and differentiation, Decaris et al. reported that producing cell-derived dECM is still challenging as the complexity of 3D constructs and culture conditions might affect the uniformity of the secreted ECM molecules on the scaffold. Obtaining a sufficient amount of cells requires in vitro expansions, and it is considered impractical and might affect the quality of the deposited ECM. In this sense, developing processing methods of solubilizing the dECM into concentrated solutions enabling the production of ECM on a large scale while still retaining their active biomolecules would significantly increase the practical application of the materials. Solubilized dECM retaining bioactive molecules could be homogeneously coated onto biomaterials and tissue engineering scaffolds with having modifiable properties.

Here, we solubilized MC3T3-E1-derived dECM using a various solubilizing reagent, and bone marrow human mesenchymal stem cells (hMSCs) were cultured on each differently solubilized dECM to compare their osteogenic potentials. To observe solubilized ECM's osteogenic potentials in a 3D culture environment, solubilized ECM coated composite scaffolds were developed. As poly(lactic-co-glycolic acid) (PLGA) and hydroxyapatite nanoparticles (HA) composite scaffolds were used as biomaterials for various bone tissue engineering application, PLGA and HA composite scaffolds were fabricated using porogen leaching method [24-27]. Furthermore, polydopamine solutions (PDA) were coated to the composite scaffold prior to the solubilized ECM coating in order to improve solubilized ECM's coating efficiency to the scaffolds. The goal of this study was to provide osteoconductive and osteoinductive properties to the composite scaffolds by applying them with solubilized dECM.

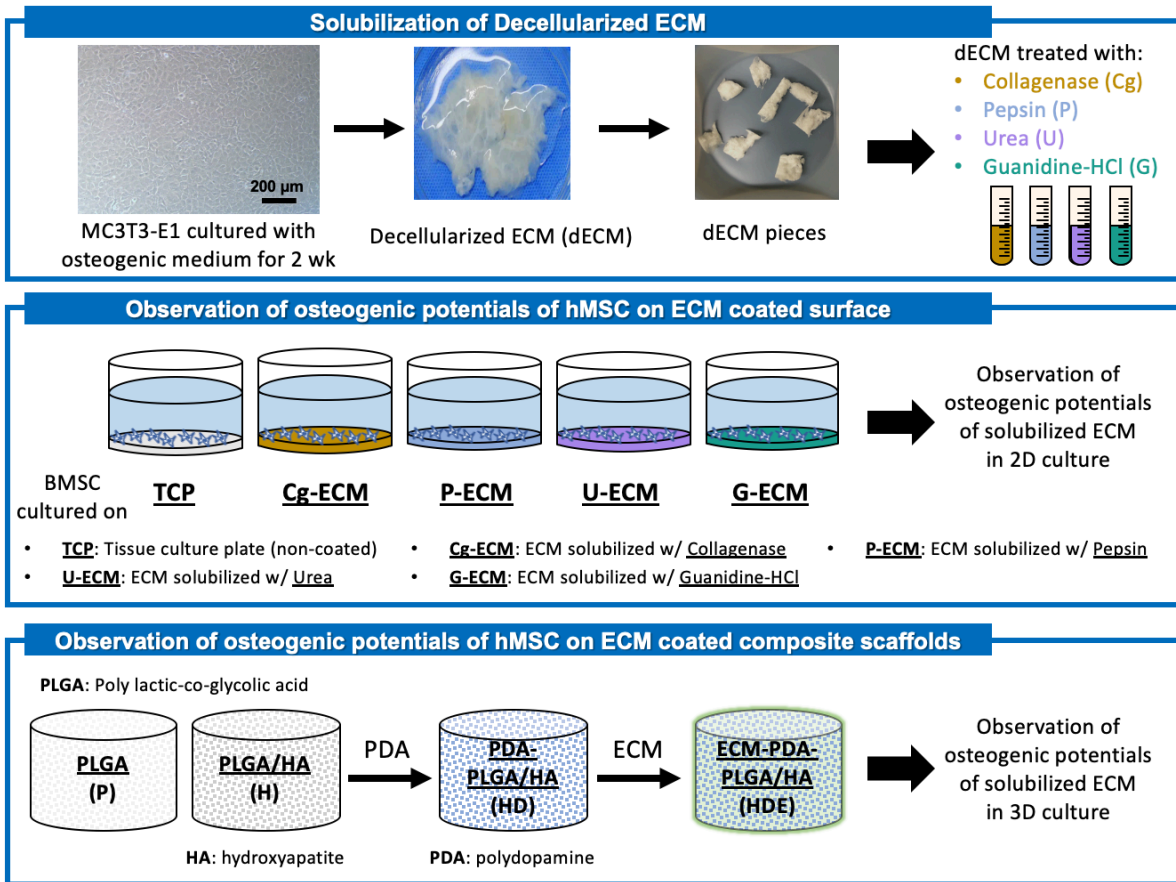


**Figure 1.** Schematic diagram of the research

## **2. Materials and methods**

### **2.1 Preparation of dECM**

The murine MC3T3-E1 (subclone 4, ATCC) were seeded in the density of  $1 \times 10^5$  cells on a 75 cm<sup>2</sup> flask with MC3T3-E1 growth medium, which consists of alpha-MEM (Gibco) supplemented with 10% fetal bovine serum (FBS; Biowest) and 1% penicillin-streptomycin (PS; Sigma). As they reached 80% of confluency, osteogenic differentiation was induced by replacing with osteogenic differentiation medium containing alpha-MEM (Gibco) supplemented with 10% FBS, 1% PS, 50  $\mu$ M ascorbic acid (Sigma), and 10 mM  $\beta$ -glycerophosphate (Sigma). After 14 days of culture with osteogenic differentiation medium, the ECM layer was detached from the flask and treated with 0.25% Trypsin-EDTA (TE; Gibco) for 1 minute. The detached ECM layer was washed with phosphate buffer saline (PBS; Welgene) and treated with 0.1% Triton X-100 in PBS for 10 minutes. The ECM sheets were washed with distilled water for 1 hour and treated with 100 U/mL DNase I (ThermoFisher) for 1 hour to remove DNA contaminants. ECM aggregates were subsequently frozen at -80°C overnight prior to lyophilization and stored at -80°C for further use.

## 2.2 Solubilization of dECM

Each of the 5 mg dECM sheets was solubilized using different solubilizing reagents, including collagenase (Worthington), pepsin from porcine gastric mucosa (Sigma), urea (Samchun), and guanidine-HCl (Sigma). For collagenase digested ECM (Cg-ECM), dECM was incubated with 200 U/ml collagenase at 37°C for 24 hours, and 1 mg/ml phosphoramidon disodium salt (Sigma) was added to inhibit further digestion from collagenase. For pepsin digested ECM (P-ECM), the dECM sheet was incubated with 0.1% pepsin (w/v) in 0.01 N HCl at 37°C for 24 hours, and 0.1 M NaOH was added to deactivate the pepsin. For urea solubilized ECM (U-ECM), the dECM sheet was incubated with 2 M Urea in 150 mM NaCl solution at 4°C for 48 hours. For guanidine-HCl solubilized ECM (G-ECM), the dECM sheet was incubated with 4 M guanidine-HCl, 50 mM sodium acetate (Sigma), 25 mM ethylenediaminetetraacetic acid (EDTA; Sigma) in PBS at 4°C for 48 hours. All differently digested/solubilized dECM are dialyzed against PBS and stored at -20°C for further use. Protein concentration of differently solubilized dECM was determined using Pierce BCA Protein Assay Kit (ThermoFisher).

## **2.3 Coating of tissue culture plates with dECM**

The 24-well plates (Eppendorf, Germany) were coated with 50  $\mu\text{g/ml}$  of Cg-ECM, P-ECM, U-ECM, and G-ECM and incubated for 1 hour at 37°C. The coated surfaces were washed with PBS before cell seeding to remove excessive molecules of dECM.

## **2.4 hMSCs culture and osteogenic differentiation**

Human bone marrow-derived MSCs (Lonza) were seeded in the density of  $1 \times 10^4$  cells on dECM-coated 24-well plates with MSC growth medium (MSCGM; Lonza) supplemented with 100  $\mu\text{g/ml}$  Primocin (InvivoGen) until they reached 80% of confluency. At confluent, osteogenic differentiation was induced by replacing with osteogenic differentiation medium, consisting of DMEM (Biowest) supplemented with 10% FBS, 1% PS, 50  $\mu\text{M}$  ascorbic acid, 10 mM  $\beta$ -glycerophosphate, and 100 nM Dexamethasone. The osteogenic differentiation medium was replaced every 2 days. For 3D culture,  $5 \times 10^4$  hMSCs were seeded on prepared scaffolds and incubated at  $37^\circ\text{C}$  with 5%  $\text{CO}_2$  for 2 hours for cell attachment on scaffolds. Scaffolds were transferred to 24-well plates and cultured with MSC osteogenic differentiation medium.

## **2.5 Cell proliferation assay**

The proliferation abilities of hMSCs for 1, 3, 5, and 7 days were determined by cell counting kit-8 (CCK-8; Dojindo).  $1 \times 10^4$  of hMSCs were seeded into a 96-well plate (Eppendorf, Germany) with MSCGM and incubated for 24 hours. The optical density was observed after 1, 3, 5, and 7 days from culture. At each time point of the experiments, 10% CCK-8 reagent solution was added to each well of the plate, and the plate was incubated for 2 hours. The optical density was obtained by measuring the absorbance at 450 nm using the microplate reader (Tecan, Switzerland). To measure the proliferation abilities of scaffolds,  $5 \times 10^4$  of hMSCs were seeded on each scaffold and measure, in the same way, using CCK-8 kit.

## 2.6 ALP and ARS staining

Alkaline phosphatase (ALP) staining and alizarin red S (ARS) staining were conducted on hMSCs differentiated in osteogenic differentiation medium for 7, 14, and 21 days and 14 and 21 days respectively to evaluate the osteogenic potentials. hMSCs were washed with phosphate buffer saline (PBS; Welgene). For ALP staining, the mixture of acetone (Aldrich) and citrate solution (Sigma) in 3:2 (v/v) was used as a fixative solution. After fixation for 1 minute, wells were washed with PBS, and ALP staining solution (0.1% naphthol AS-MX phosphate (Sigma-Aldrich) and 0.1% fast blue BB salt (Sigma)) was treated for 30 minutes at room temperature in the dark. Then, wells were washed with PBS for 1 minute. To measure the ALP activities, alkaline phosphate assay kit (Abcam) was used according to the manufacturer's protocol. Briefly, hMSCs cultured for different time points were lysed, and p-nitrophenol, which was released from p-nitrophenyl phosphate (pNPP), were measured at 405nm using a microplate reader. For ARS staining, cells were fixed with 4% paraformaldehyde (PFA; Biosesang) in PBS for 5 minutes and washed with distilled water. Then, 2% ARS (w/v) (Sigma) in distilled water was added to the wells and incubated for 10 minutes. Subsequently, wash wells with distilled water for 10 minutes. To quantify the mineralization abilities, stained cells were incubated with 10% cetylpyridinium chloride solution in distilled water for 30 minutes, and the absorbance intensities were measure at 545 nm using the microplate reader. All images of stained results were obtained using an optical microscope (Olympus).

## 2.7 qRT-PCR on osteogenic marker gene

hMSCs were cultured on various solubilized ECM and porous scaffolds for 7, 14, and 21 days to measure the expression levels of the osteogenic markers of the hMSCs, including runt-related transcription factor 2 (RUNX2), osteopontin (OPN), and osteocalcin (OCN). At each time point, the cells were digested, and total RNA was isolated. The cDNA was then synthesized using a Superscript III first-strand synthesis kit (ThermoFisher) according to the manufacturer's protocol. The expression of osteogenic markers was quantified by qPCR SYBR Green (Bioline). Gene-specific primers, including glyceraldehyde-3-phosphate dehydrogenase (GAPDH), runt-related transcription factor 2 (RUNX2), osteopontin (OPN), and osteocalcin (OCN), were designed using NCBI Primer-BLAST. qRT-PCR was conducted by StepOnePlus Real-Time PCR system (Applied Biosystems), and the relative gene expression levels of RUNX2, OPN, and OCN were normalized to that of GAPDH. All experiments were done in triplicate to obtain average data.

The gene-specific primers were as follows: human GAPDH (Forward: 5'-ATG GGG AAG GTG AAG GTC G-3', reverse: 5'-GGG GTC ATT GAT GGC AAC AAT A-3'), human RUNX2 (Forward: 5'-TGG TTA CTG TCA TGG CGG GTA-3', reverse: 5'-TCT CAG ATC GTT GAA CCT TGC TA-3'), human OPN (Forward: 5'-CAC TAC CAT GAG AAT TGC AGT GA-3', reverse: 5'-CTG CTT TTC CTC AGA ACT TCC A-3'), and human OCN (Forward: 5'-TGA GAG CCC TCA CAC TCC TC-3', reverse: 5'-CGC CTG GGT CTC TTC ACT AC-3')

## **2.8 Fabrication of HA-coated paraffin spheres**

The HA nanoparticle-coated paraffin spheres were prepared using the Pickering emulsion method [28]. Briefly, 0.8 g of the hydroxyapatite nanoparticles were homogeneously dispersed in 40 ml of distilled water. Then, 4 g of paraffin wax was added at 80°C and stirred at 900 rpm for 30 minutes. The paraffin microspheres were solidified by pouring ice-cold water into the solution. To remove weakly bound HA particles, the paraffin spheres were washed with distilled water twice. Dried HA-coated paraffin spheres were collected and sieved to a size of 200-400  $\mu\text{m}$ . HA-coated paraffin spheres were stored in a desiccator for further use. For comparison, paraffin spheres were fabricated with the same method by using poly(vinyl alcohol) as the emulsifier.

## **2.9 Fabrication of PLGA/HA scaffolds**

The HA-coated paraffin spheres in a size range between 200-400  $\mu\text{m}$  were packed into a mold (a cylindrical shape with a diameter of 5 mm and a height of 2 mm). To produce good pore interconnectivity, HA-coated paraffin spheres were bound together by sintering scaffolds at 45°C for 30 minutes. After cooling scaffolds to room temperature, 30  $\mu\text{l}$  of 12% PLGA/1,4-dioxane solution was cast onto the mold in a dropwise manner. Then, scaffolds were subsequently frozen at -25°C for 2 hours and followed by lyophilization to remove 1,4-dioxane. The PLGA/HA porous scaffolds were finally obtained by leaching the paraffin with hexane at room temperature for 2 days. The hexane was replaced every 6 hours. For group comparison, pure PLGA scaffolds were also produced in the same way using pure paraffin spheres.

## **2.10 Polydopamine and G-ECM coating on the scaffold**

Prepared scaffolds, including pure PLGA scaffolds and PLGA/HA scaffolds, were coated with polydopamine (PDA) solutions, as previously described [29]. Briefly, the dried scaffolds were immersed in an aqueous polydopamine solution (2 mg/ml dopamine in 10 mM Tris-HCl, pH = 8.5) with agitation at room temperature for 2 hours. Then the PDA-coated scaffolds were washed with distilled water five times to remove unbound dopamine molecules. Subsequently, the G-ECM were immobilized onto scaffolds by immersing scaffolds in a G-ECM solution (1  $\mu\text{g/mL}$  in PBS) with shaking at 4°C for overnight. Finally, the PDA-coated and G-ECM immobilized scaffolds were washed three times with distilled water. For all experiments, the dimension of cylindrical porous scaffolds of 5 mm in length and 2 mm in height were used.

## **2.11 Characterization of spheres and scaffolds**

The spheres' with a size range of 200-400 nm and cylindrical porous scaffolds with 5 mm in length and 2 mm in height were used for all experiments. Four different types of scaffolds, including PLGA scaffold (P), PLGA/HA scaffold (H), PDA-coated PLGA/HA scaffold (HD), and G-ECM and PDA coated PLGA/HA (HDE), were characterized. The surface morphology of the spheres and scaffolds was observed by a field emission scanning electron microscopy (FE-SEM) using JSM-7800F Prime (JEOL). Also, energy-dispersive spectroscopy (EDS) analysis and fourier transform infrared spectroscopy (FTIR; Perkin Elmer) were used to evaluate the elemental composition and chemical composition of the spheres and scaffolds.

## 2.12 Statistical analysis

All experiments were conducted at least 3 times ( $n \geq 3$ ) unless otherwise stated. All quantitative data were presented as mean  $\pm$  standard error of the mean. One-way ANOVA with Turkey's multiple comparison tests was performed using GraphPad Prism software. Asterisk indicates a significant difference at \* $P < 0.05$ ; \*\* $P < 0.01$ ; \*\*\* $P < 0.001$ .

### **3. Results and discussion**

#### **3.1 Production of decellularized ECM and solubilized dECM**

The production of MC3T3-E1-derived decellularized ECM and solubilization of dECM are schematically illustrated in Figure 1. The dECM was treated with various solubilizing reagents to produce collagenase-digested dECM (cg-ECM), pepsin-solubilized dECM (P-ECM), urea-solubilized dECM (U-ECM), and guanidine-HCl-solubilized dECM (G-ECM). The protein concentrations of each solubilized dECM were determined (Table 1). The protein concentration of cg-ECM was significantly lower than in other groups. The low protein concentration of cg-ECM could be explained by the previous study from Kuljianin et al. that treating collagenase could deplete collagen from ECM-derived protein extracts by reducing its relative abundance from up to 90% to below 10% [30]. G-ECM had the highest protein concentration. It might be the indication of guanidine-HCl extracts ECM with a relatively high abundance of proteins compared to other reagents.

**Table 1.** The protein concentrations of solubilized dECM

Solubilized ECM	CG-ECM	P-ECM	U-ECM	G-ECM
Protein Concentration ( $\mu\text{g/ml}$ )	$67.39 \pm 62.09$	$213.56 \pm 32.34$	$245.12 \pm 42.46$	$277.85 \pm 34.07$

### **3.2 G-ECM coating induces cell proliferation and osteogenic differentiation of hMSCs.**

Several solubilization methods were utilized to observe their cell proliferation and differentiation abilities to account for its different ECM protein compositions from various solubilization methods [18, 31]. The CCK assay was conducted to evaluate proliferation abilities of hMSCs cultured on differently solubilized dECM at 1, 4, 7, and 10 days of culture. As shown in Figure 2, hMSCs cultured on G-ECM exhibited the highest proliferation abilities at all time points than other groups. The results showed that G-ECM promotes the proliferation of hMSCs, even at the early stage of growth. To evaluate the osteogenic differentiation of hMSCs on various solubilized dECM, ALP activities, and calcium deposition from ARS staining and quantification were measured (Figure 3 and 4). As the microscopic analysis of stained images in Figure 3a and 4a illustrates that G-ECM groups were the most brightly stained group. Data in Figure 3b and 4b also showed that the highest ALP activities and ARS absorbance were evaluated on the G-ECM group at all time points. Besides, the expression levels of osteogenic marker genes were compared among different ECM groups (Figure 5). The relative expression levels of RUNX2, OPN, and OCN on G-ECM showed the greatest among others. These results indicate that dECM solubilized with guanidine-HCl facilitates cell proliferation and induces osteogenic differentiation.

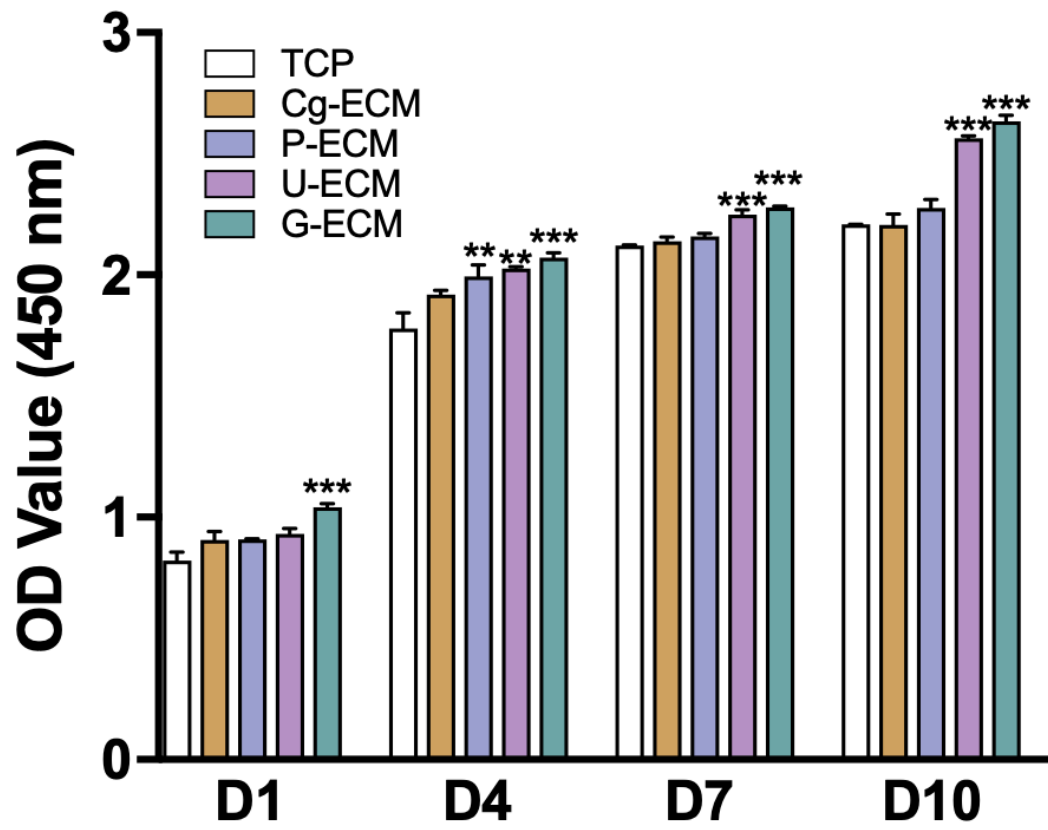


**Figure 2.** Proliferation abilities of hMSCs cultured on differently solubilized dECM measured at day 1, 4, 7, and 10

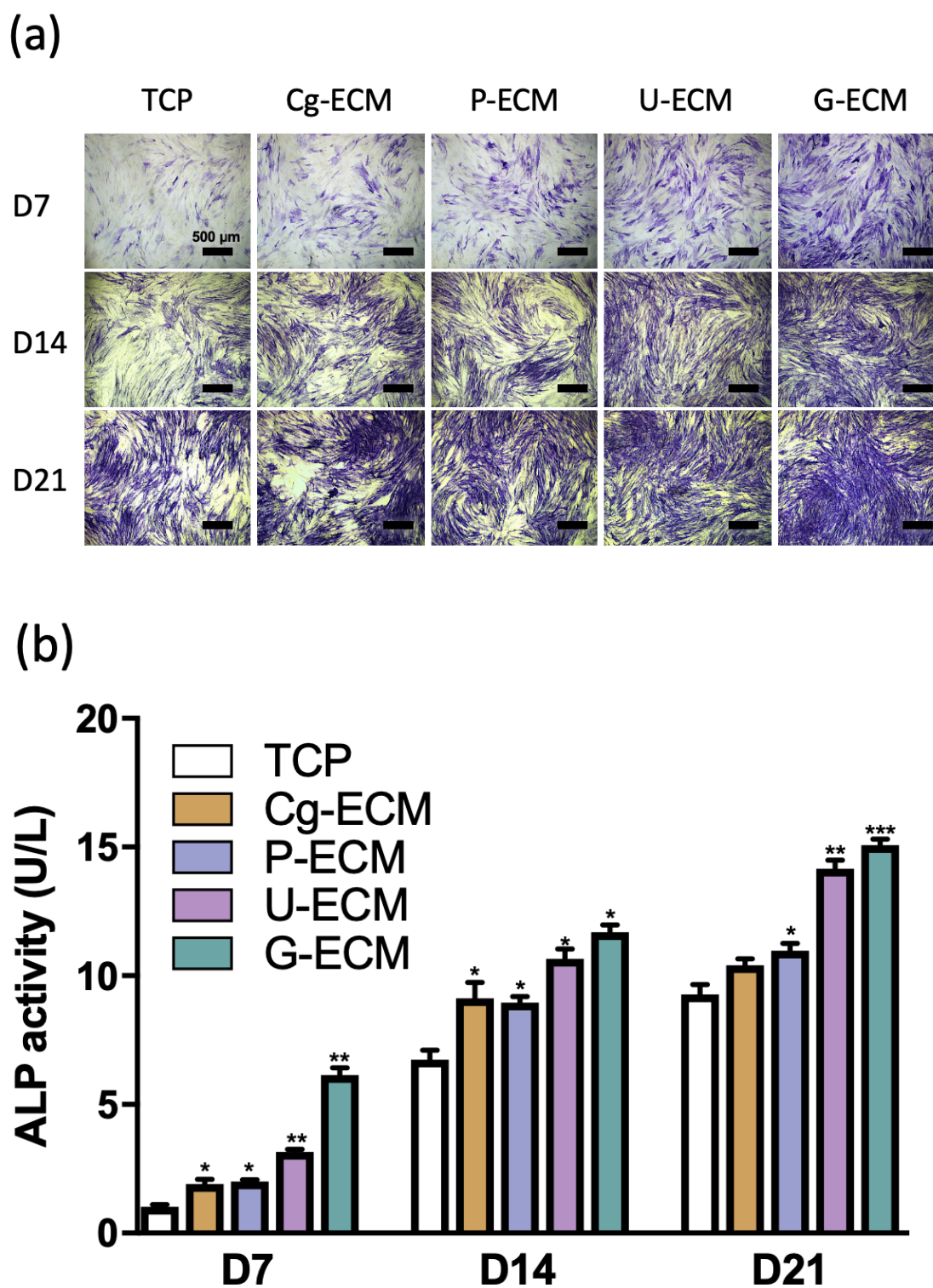
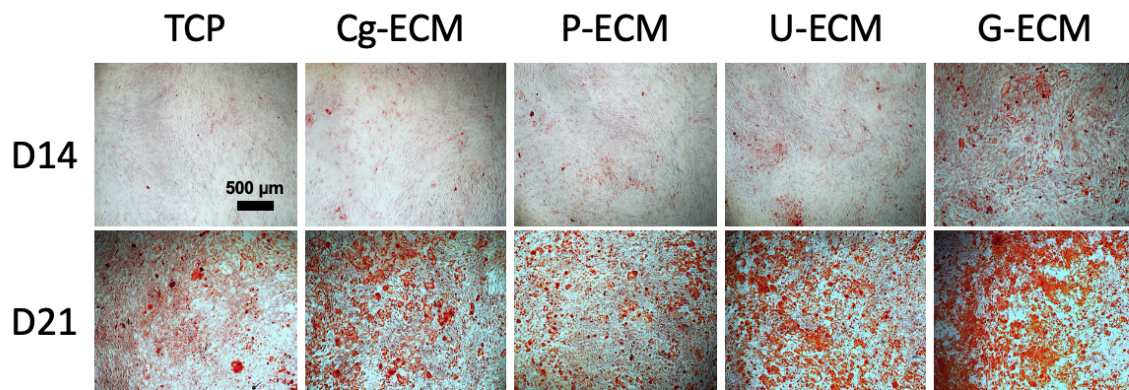


**Figure 3.** (a) ALP activities staining and (b) quantification results of hMSCs cultured on differently solubilized dECM at day 7, 14, and 21

(a)



(b)

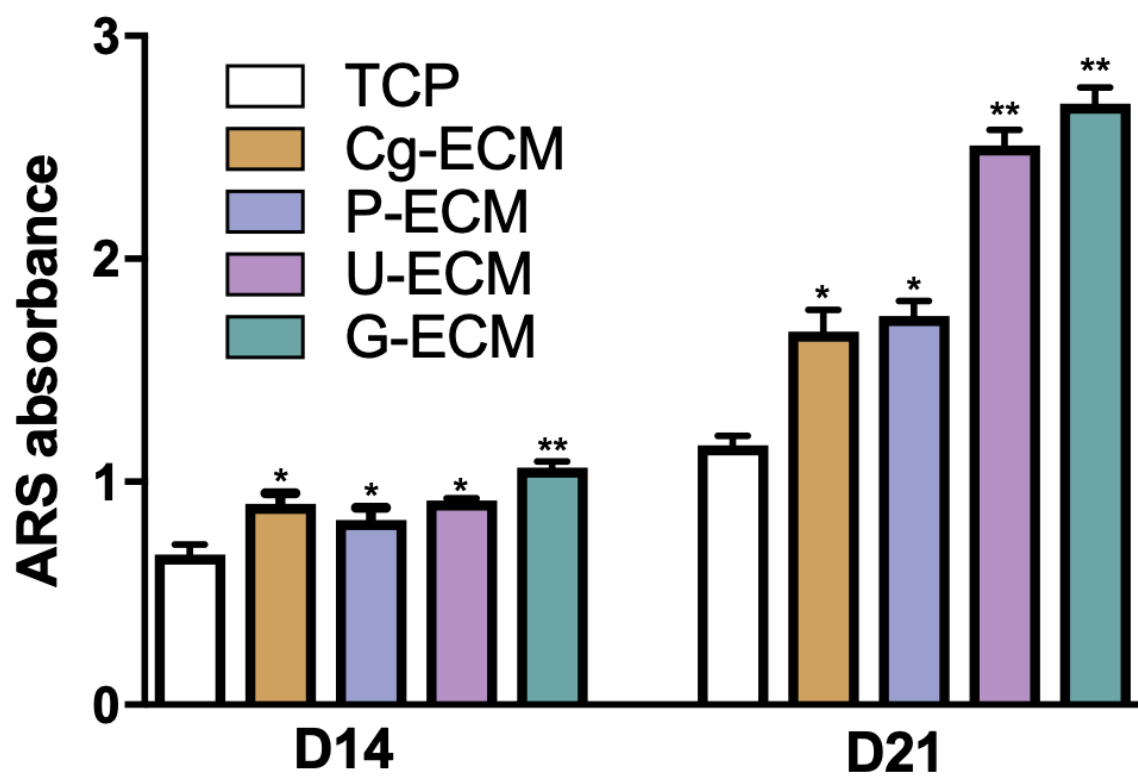


**Figure 4.** (a) ARS staining and (b) quantification results of hMSCs cultured on differently solubilized dECM at day 14, and 21

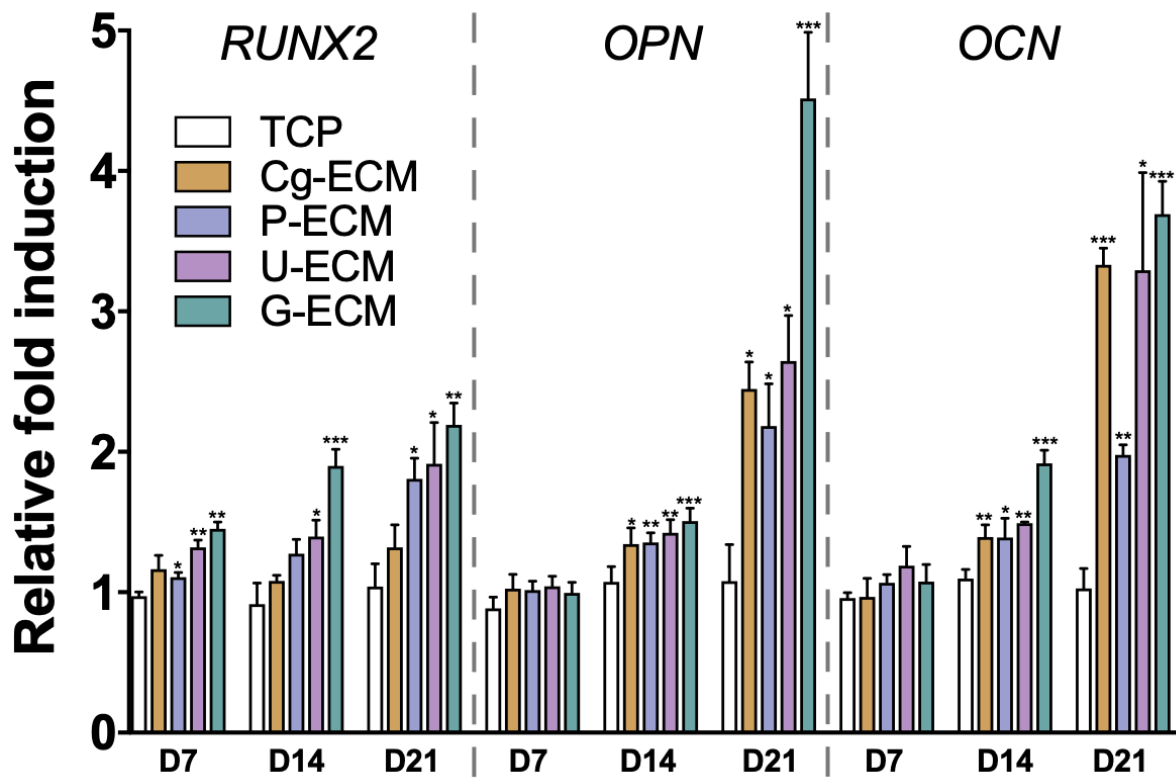
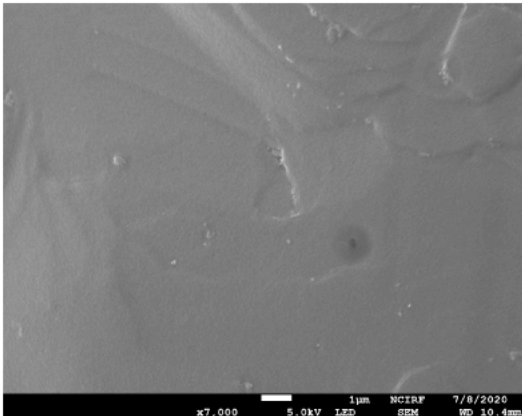
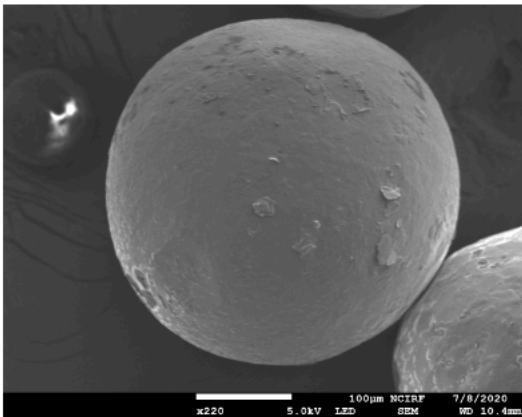
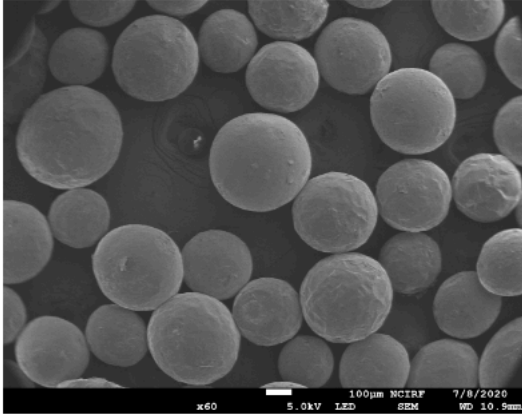


**Figure 5.** Expression levels of osteogenic marker genes of hMSCs cultured on differently solubilized dECM at day 7, 14, and 21

### **3.3 Fabrication and characterization of HA-coated paraffin spheres**

Paraffin spheres covered with hydroxyapatite were prepared using the Pickering method. The SEM images shown in Figure 6 indicate that paraffin spheres were well fabricated in the desired size range of 200-400  $\mu\text{m}$ . Compared with the pure paraffin spheres' smooth surface, the HA-coated paraffin spheres possessed a rougher surface morphology. These results indicate that HA is embedded on the surface of the paraffin spheres. To further confirm the presence of HA-coated surface, EDS and FTIR analysis were conducted (Figure 7 and 8). From the EDS spectrum of HA-coated paraffin sphere, peaks representing calcium and phosphorus ions were showed in Figure 7b, while no peaks are shown in the EDS spectrum of pure paraffin sphere (Figure 7a). FTIR spectra also revealed phosphate peak only in the spectrum of HA-coated paraffin spheres (Figure 8b). SEM images, EDS, and FTIR analysis altogether confirmed that HA nanoparticles were coated on the surface of the paraffin spheres.

## Paraffin spheres



## HA-coated paraffin spheres

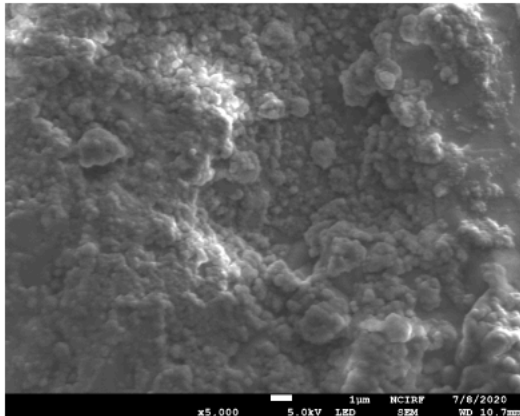
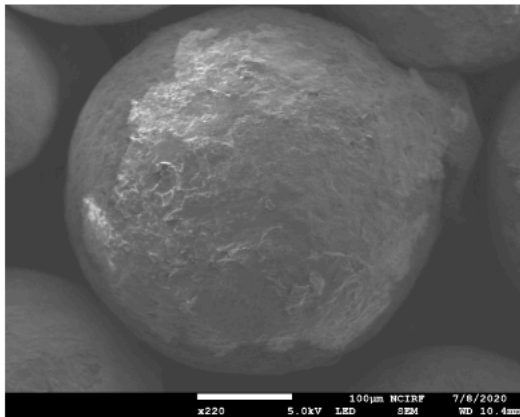
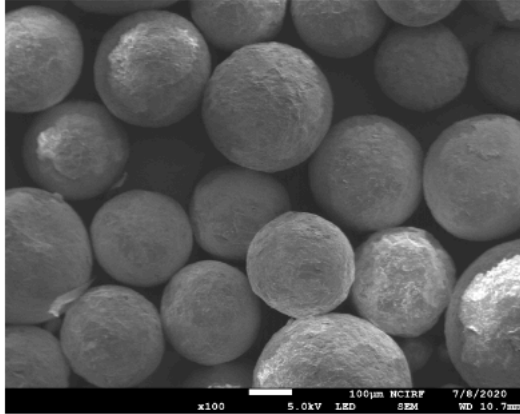
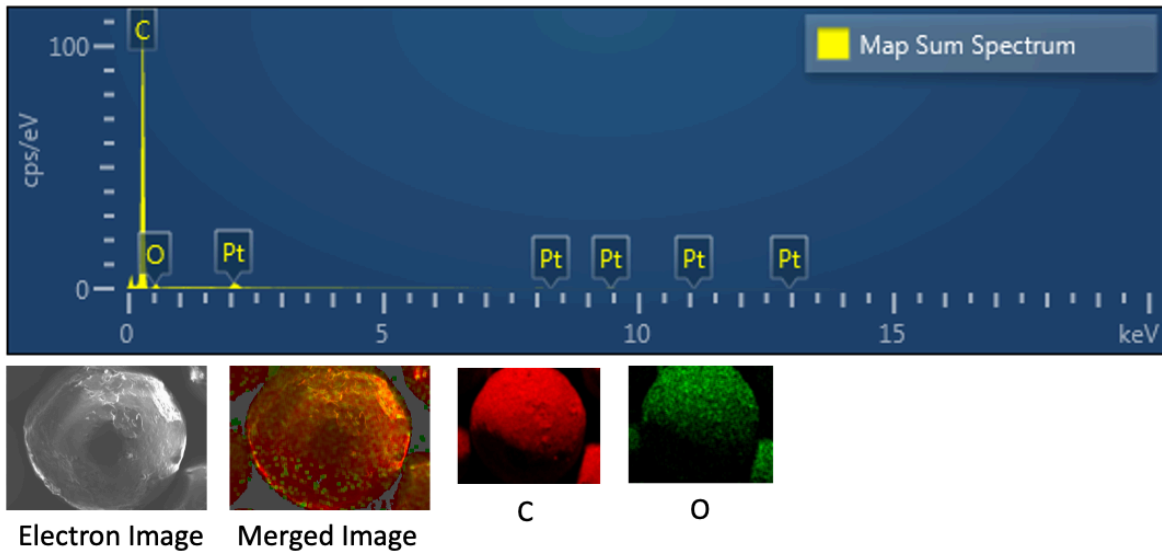


**Figure 6.** SEM images of paraffin and HA-coated paraffin spheres

### (a) Paraffin spheres



### (b) HA-coated paraffin spheres

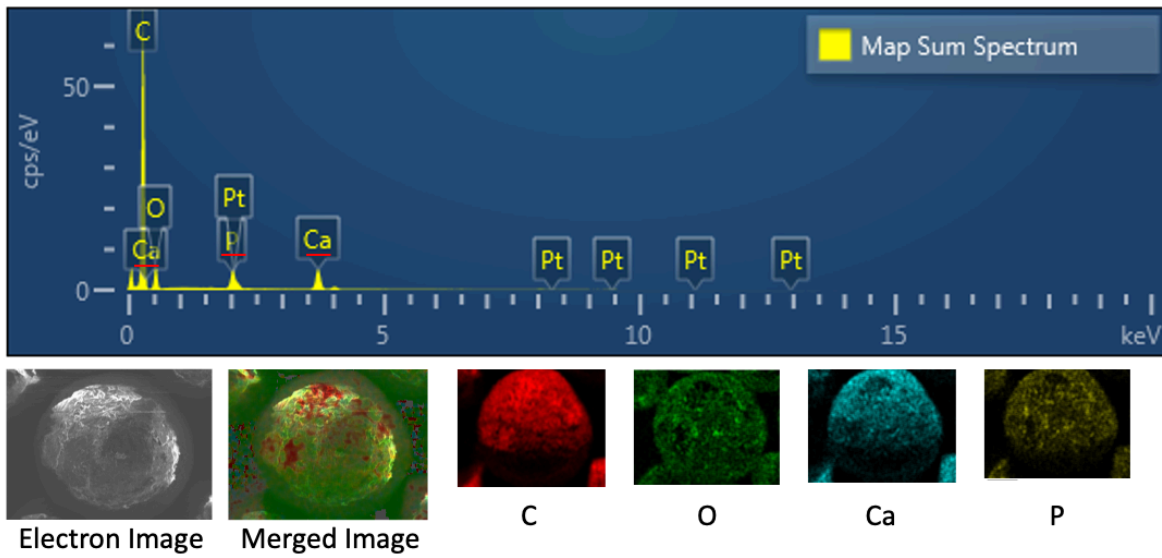


**Figure 7.** EDS analysis of (a) paraffin and (b) HA-coated paraffin spheres

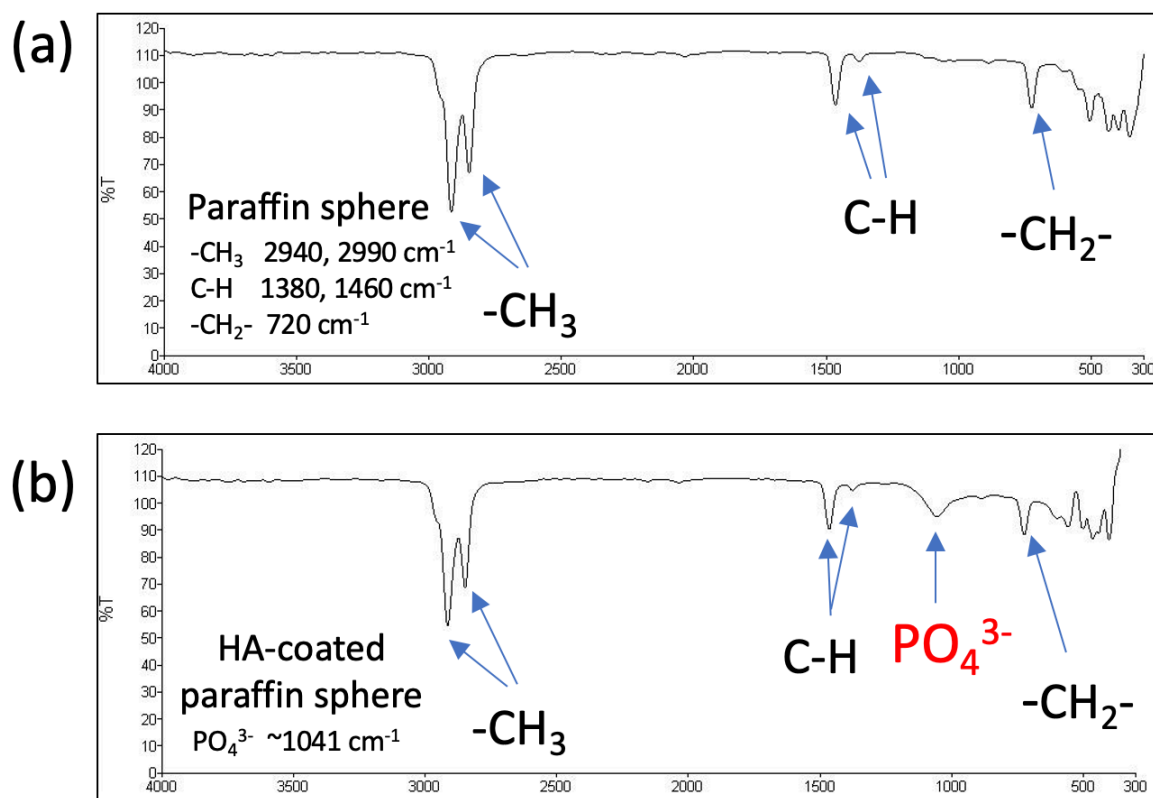


**Figure 8.** FTIR analysis of (a) paraffin and (b) HA-coated paraffin spheres

### 3.4 Fabrication and characterization of the scaffolds

Four different types of scaffolds, including PLGA scaffold (P), PLGA/HA scaffold (H), PDA-coated PLGA/HA scaffold (HD), and G-ECM and PDA coated PLGA/HA (HDE), were fabricated. Pure paraffin spheres and HA-coated paraffin spheres were used as porogens, and P and H scaffolds were fabricated using the porogen leaching method [28]. Further fabrication of HD and HDE scaffolds was conducted by coating polydopamine solutions and G-ECM, respectively. To improve G-ECM's coating efficiency, PDA was coated before G-ECM coating [32]. As shown in Figure 9a, PLGA (P), PLGA/HA (H), PDA-PLGA/HA (HD), and G-ECM-PDA-PLGA/HA (HDE) were fabricated with good pore interconnectivity. The diameter of these pores ranged from 200 to 400  $\mu\text{m}$ , which was matched with the size of the paraffin spheres. The rough surface of scaffolds was found from a detailed examination of scaffolds' pore surface using SEM images (Figure 9b). This indicates that HA nanoparticles are well embedded on the pore surface. To confirm the presence of HA and PDA coating on the scaffold, EDS and FTIR analysis were conducted (Figure 10 and 11). Peaks representing calcium and phosphorus ions were clearly shown in Figure 10b and 10c, while those peaks are not shown in the P scaffold's EDS spectrum (Figure 10a). In the merged image in Figure 10b, the bluish-purple colors were explicitly shown in the scaffold's pore surface, indicating that HA nanoparticles are well incorporated on the scaffold's pore surface. In Figure 10C, the nitrogen ion peak found in EDS spectrum of the HD scaffold indicates PDA solution was well coated on the HD scaffold. FTIR spectra also revealed the presence of phosphate peak at 570  $\text{cm}^{-1}$  and the primary amine peak at 1600  $\text{cm}^{-1}$  in the spectra of H and HD scaffolds (Figure 11b and 11c). From SEM images, EDS, and FTIR analysis, it is clear that HA nanoparticles and PDA are well incorporated and coated on the scaffold.

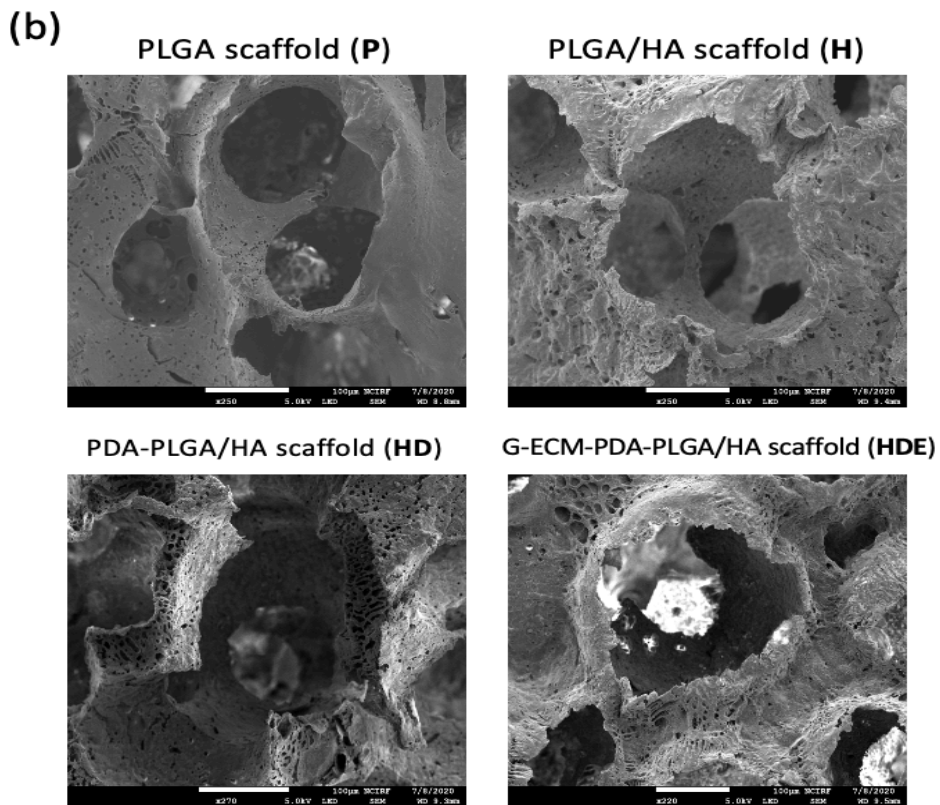
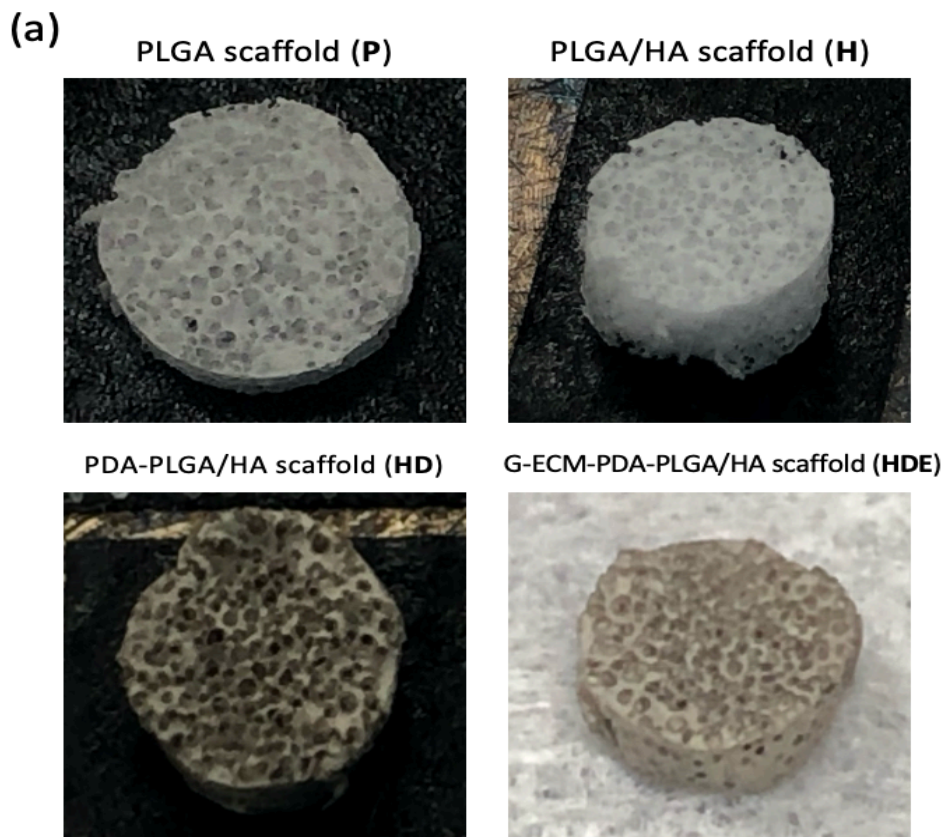
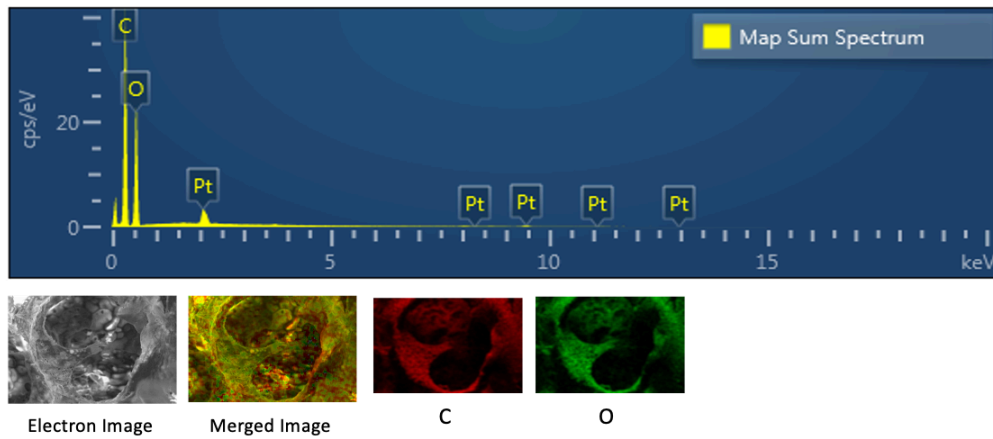
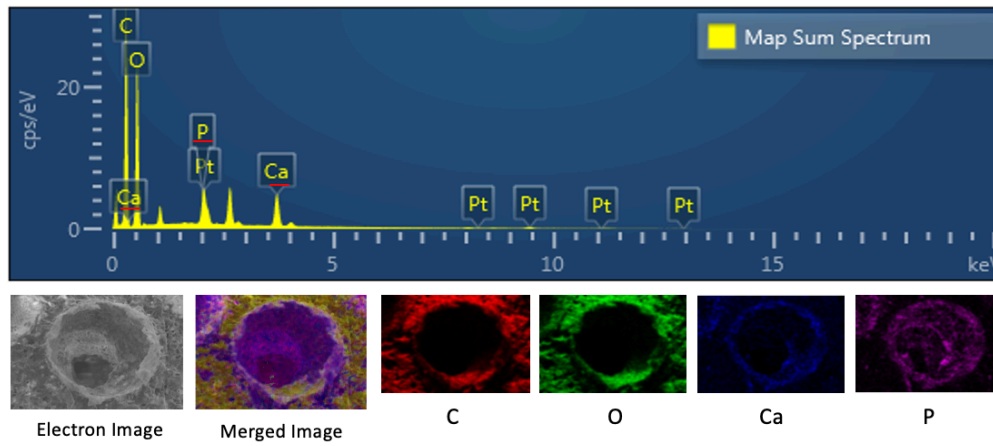


**Figure 9.** (a) Optical and (b) SEM images of scaffolds

**(a) PLGA scaffold (P)**



**(b) PLGA/HA scaffold (H)**



**(c) PDA-PLGA/HA scaffold (HD)**

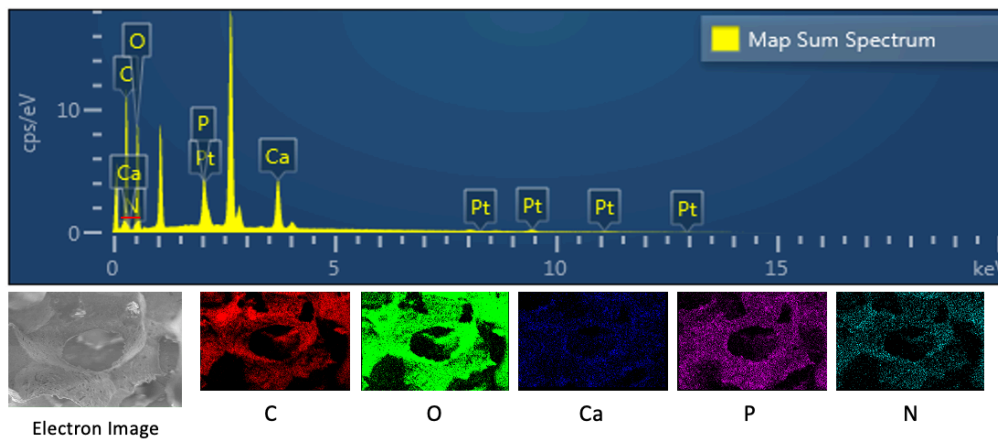


**Figure 10.** EDS analysis of (a) PLGA, (b) PLGA/HA, (c) PDA-PLGA/HA scaffolds

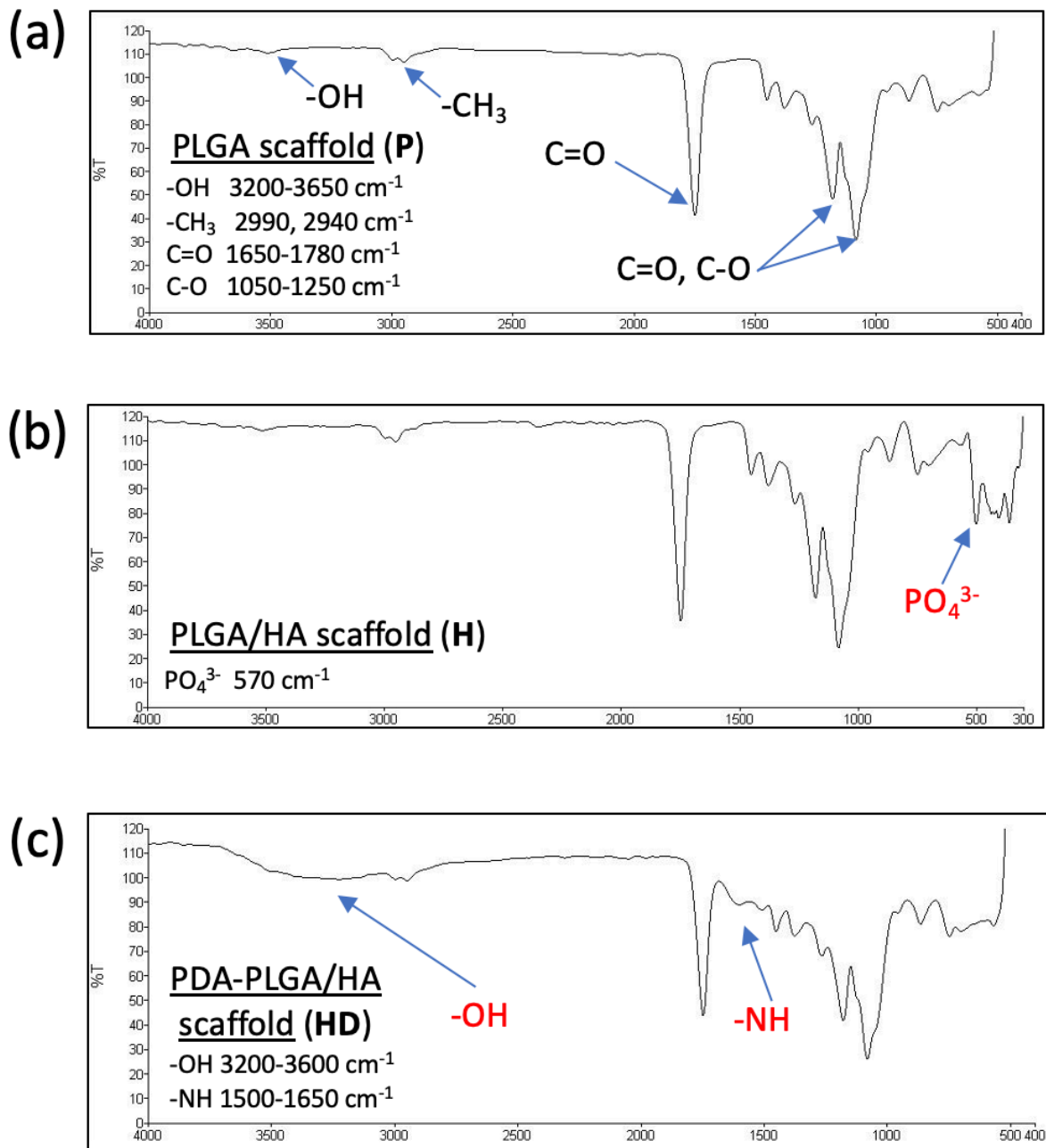


**Figure 11.** FTIR analysis of (a) PLGA, (b) PLGA/HA, and (c) PDA-PLGA/HA scaffolds

### **3.5 G-ECM composite scaffold promotes osteogenesis of hMSCs**

hMSCs were cultured on four different types of scaffolds, including PLGA (P), PLGA/HA (H), PDA-PLGA/HA (HD), and G-ECM-PDA-PLGA/HA (HDE). hMSCs proliferation abilities on scaffolds were evaluated at day 1, 3, 5, and 7 of culture, and results were shown in Figure 12. In all scaffolds, the hMSCs were able to proliferate. Although there were no significant difference at day 1, the HDE scaffolds showed improved proliferation abilities compare to other scaffolds at day 3, 5, and 7. The ALP activities and ARS staining and quantitation of hMSCs cultured on different types of scaffolds were carried out to observe the osteogenic potentials of the G-ECM on the scaffold. Besides, the expression levels of osteogenic marker genes were compared among different scaffolds. Data in Figure 13 and 14 indicates that an additional coating of G-ECM provides enhanced ALP activities and mineralization abilities. The expression levels of osteogenic marker genes were compared among four different scaffolds, and expression levels of RUNX2, OPN, and OCN were the highest in the G-ECM coated group (Figure 15). These results indicate that coating scaffold with guanidine-HCl solubilized dECM could facilitate the proliferation abilities and induce osteogenic differentiation of hMSCs.

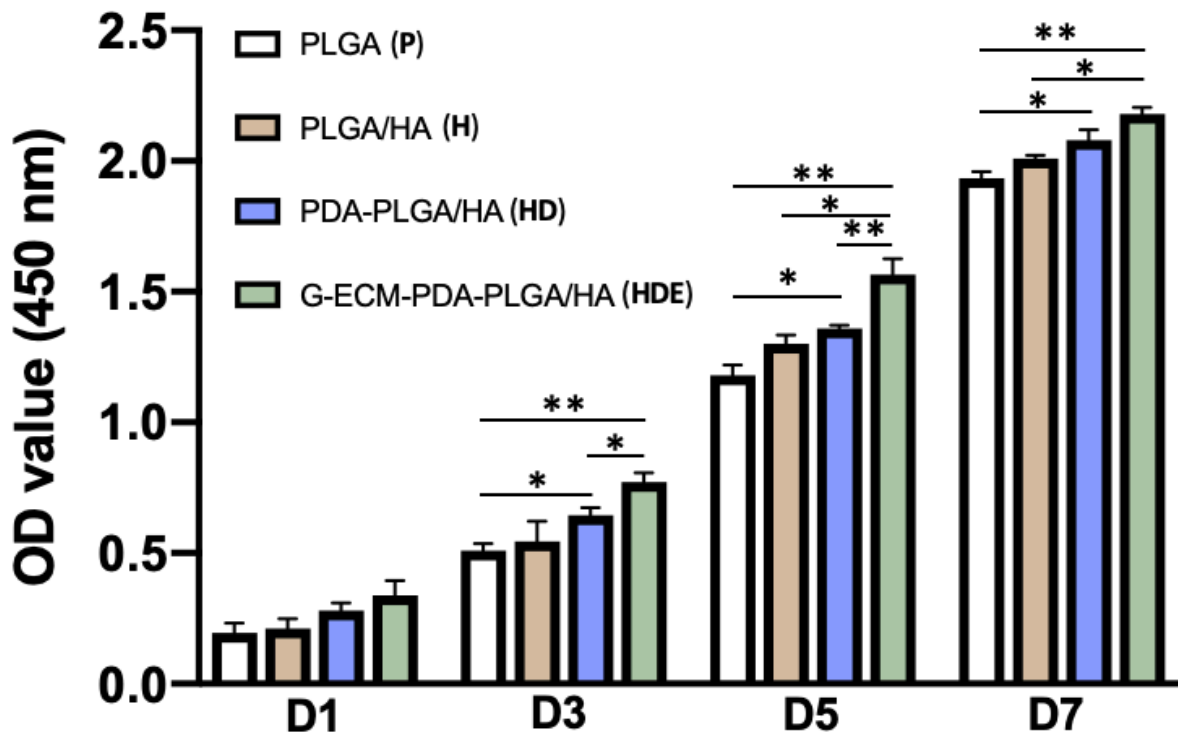


Figure 12. The proliferation of abilities of hMSCs cultured on scaffolds at day 1, 3, 5, and 7

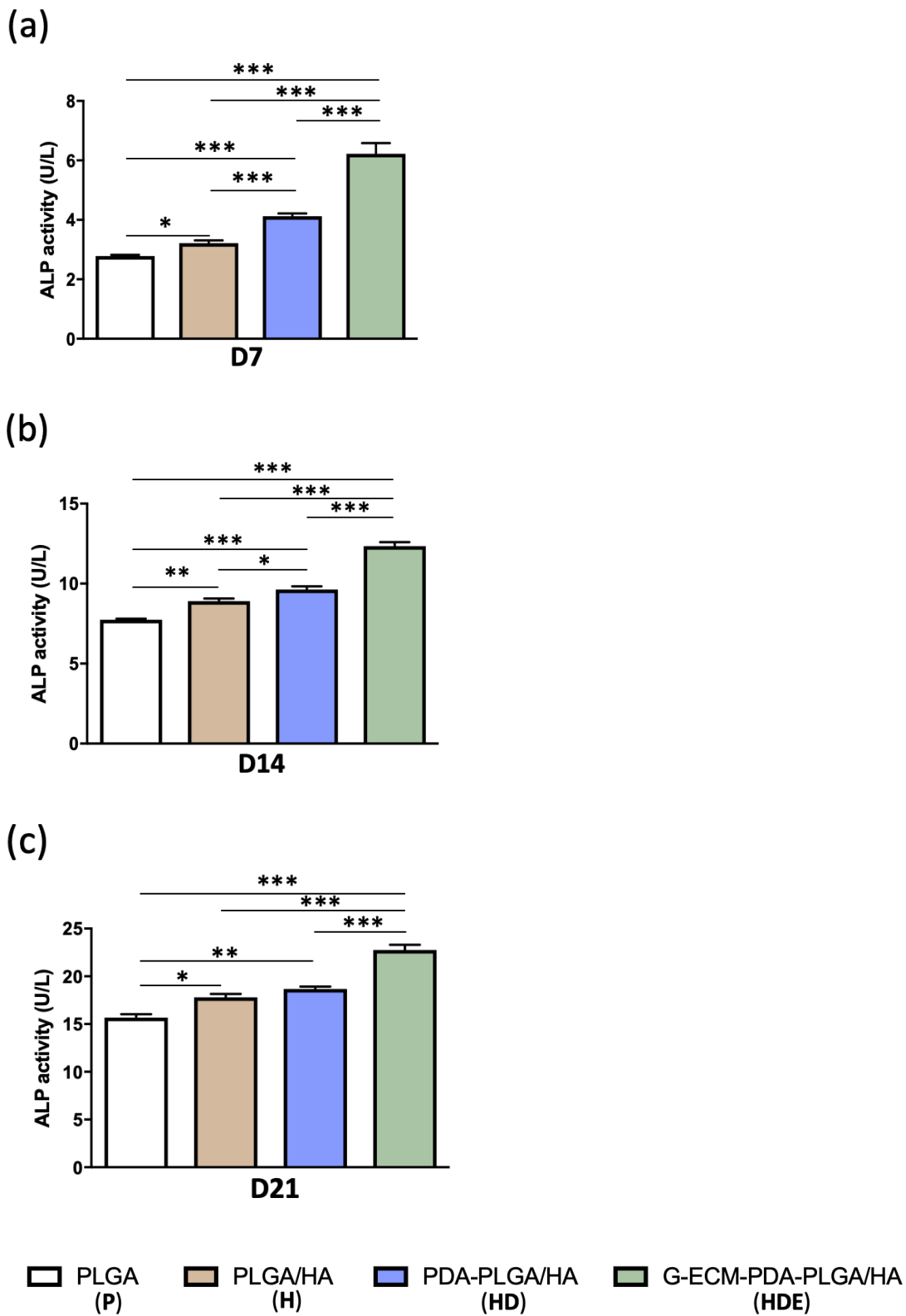
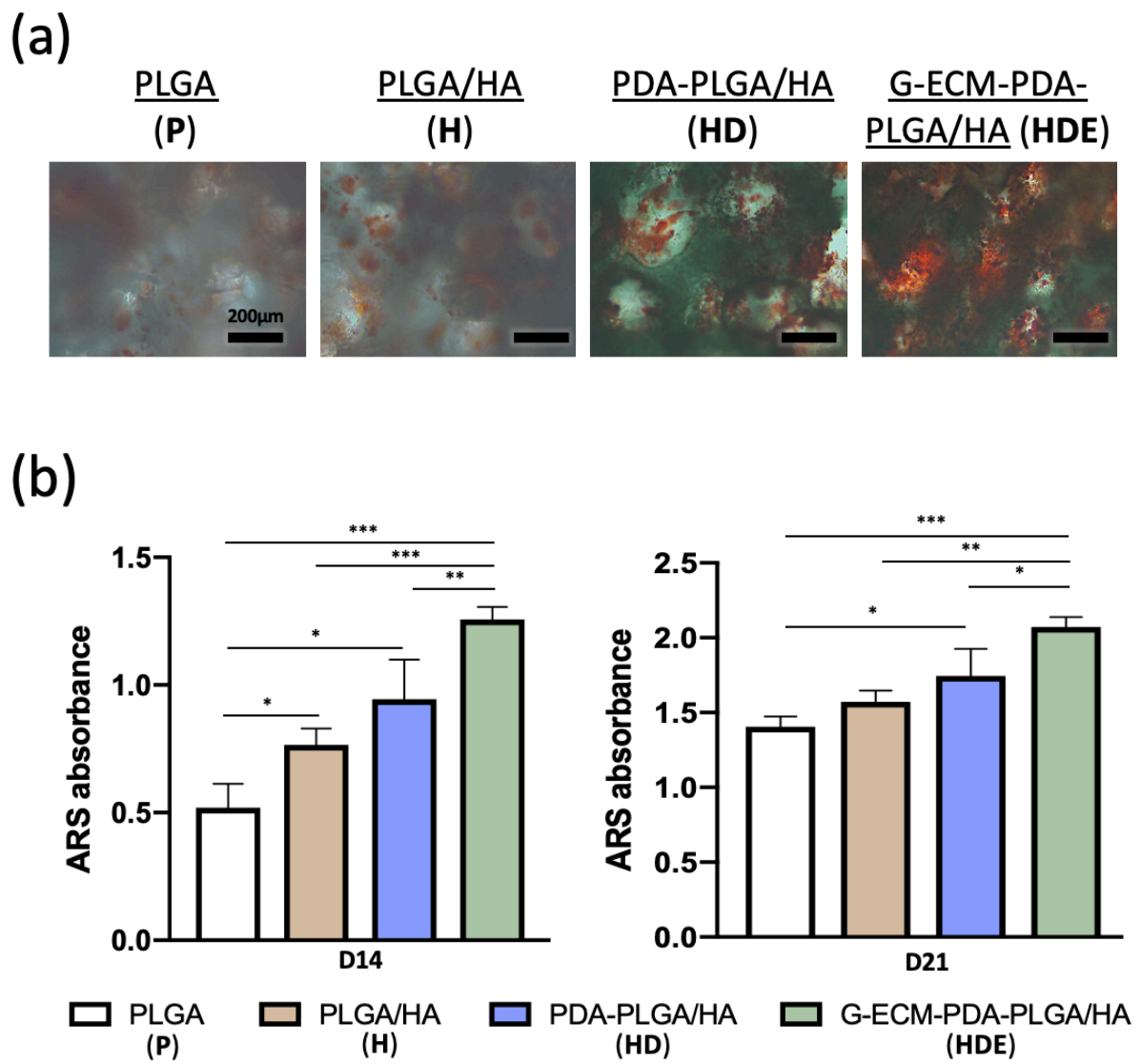
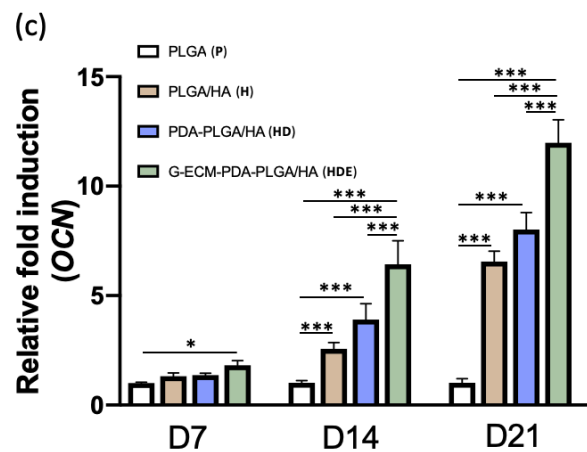
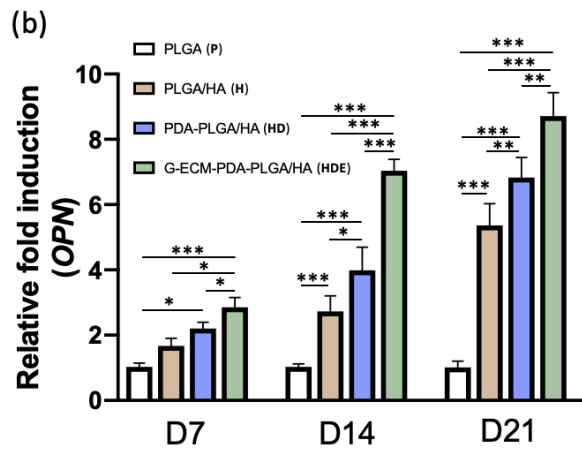
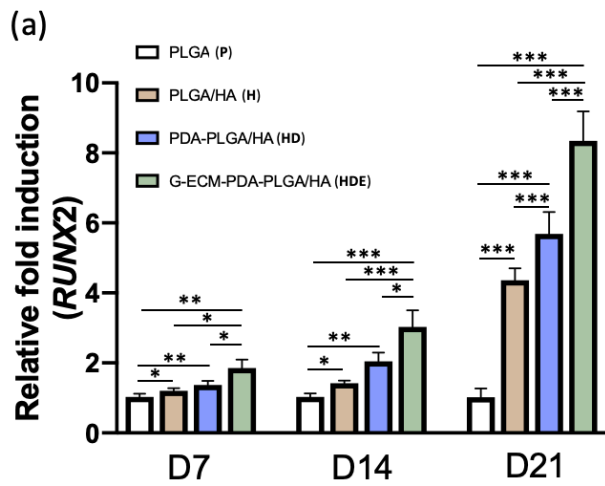


Figure 13. ALP activities of hMSCs cultured on 3D scaffolds at day (a) 7, (b) 14, and (c) 21



**Figure 14.** (a) ARS staining at day 14, and (b) ARS quantification of hMSCs on scaffolds at day 14 and 21



**Figure 15.** Expression levels of osteogenic marker genes (a) *RUNX2*, (b) *OPN*, and (c) *OCN* at day 7, 14, and 21

## 4. Conclusions

We solubilized MC3T3-E1-derived decellularized matrix using various solubilizing reagents, including collagenase, pepsin, urea, and guanidine-HCl, to evaluate dECM's osteogenic capacities. Proliferation abilities and osteogenic differentiation potentials of each solubilized dECM were assessed. Among those differently solubilized methods, dECM solubilized with guanidine-HCl (G-ECM) effectively facilitated cell proliferation at the early stage of hMSCs growth and provided strong osteogenic potentials to hMSCs. It is assumed that the improved osteogenic potentials are due to the preservation of abundant glycosaminoglycans through the guanidine-HCl solubilization method. With its confirmed osteogenic potentials, the effects of G-ECM in 3D cultures were further evaluated by developing G-ECM coated PLGA/HA composite scaffolds. The introduction of G-ECM onto the scaffold can effectively promote the expression of osteoblast-related genes and enhances proliferation and differentiation of hMSCs.

Our study demonstrates that the effective process of solubilizing dECM using guanidine-HCl provides osteogenic potentials. Furthermore, we found that coating solubilized G-ECM onto the scaffold facilitates the osteogenic differentiation of hMSCs in a 3D scaffold. Therefore, solubilize G-ECM could be utilized as osteoinductive biomaterials, and it could be a promising biomaterial in multidisciplinary research, including tissue engineering and regenerative medicine.

## 5. References

- [1] Silber, J., Anderson, D., Daffner, S., Brislin, J., Leland, J., Hilibrand, A., Vaccaro, A., Albert, T. (2003). Donor site morbidity after anterior iliac crest bone harvest for single-level anterior cervical discectomy and fusion. *Spine*, 28, 134-139.
- [2] Mankin, H., Hornicek, F., Raskin, K. (2005). Infection in massive bone allografts. *Clin. Orthop. Relat. Res.*, 432, 210-216.
- [3] Zhang, P., Hong, Z., Yu, T., Chen, X., Jing, X. (2009). In vivo mineralization and osteogenesis of nanocomposite scaffold of poly (lactide-co-glycolide) and hydroxyapatite surface-grafted with poly (L-lactide). *Biomaterials*, 30(1), 58-70.
- [4] Wei, G., Ma, P. (2004). Structure and properties of nano-hydroxyapatite/polymer composite scaffolds for bone tissue engineering. *Biomaterials*, 25(19), 4749-4757.
- [5] Fu, S., Wang, X., Guo, G., Shi, S., Liang, H., Luo, F., Wie, Y., Qian, Z. (2010). Preparation and characterization of nano-hydroxyapatite/poly ( $\epsilon$ -caprolactone)-poly (ethylene glycol)- poly ( $\epsilon$ -caprolactone) composite fibers for tissue engineering. *J. Phys. Chem. C*, 114(43), 18372-18378.
- [6] Wang, X., Zhang, G., Qi, F., Cheng, Y., Lu, X., Wang, L., Zhao, J., Zhao, B. (2018). Enhanced bone regeneration using an insulin-loaded nano-hydroxyapatite/collagen/PLGA composite scaffold. *J. Nanomed.*, 13, 117-127.
- [7] Bhuiyan, D., Middleton, J., Tannenbaum, R., Wick, T. (2017). Bone regeneration from human mesenchymal stem cells on porous hydroxyapatite-PLGA-collagen bioactive polymer scaffolds. *Biomed. Mater. Eng.*, 28, 671-685.
- [8] Zhao, X., Han, Y., Li, J., Cai, B., Gao, H., Feng, W., Li, S., Liu, J., Li, D. (2017). BMP-2 immobilized PLGA/hydroxyapatite fibrous scaffold via polydopamine stimulates osteoblast growth. *Mater. Sci. Eng. C*, 78, 658-666.
- [9] Jung, J., Bhuiyan, D., Ogle, B. (2016). Solid organ fabrication: comparison of decellularization to 3D bioprinting. *Biomater Res.*, 20(10), 20-27.
- [10] Mecham, R. (2012). Overview of extracellular matrix. *Curr. Protoc. Cell Biol.*, Chapter 57, 10.1.1-10.1.16.
- [11] Bonnans, C., Chou, J., Werb, Z. (2014). Remodelling the extracellular matrix in development and disease. *Nat. Rev. Mol. Cell Biol.*, 15, 786-801.
- [12] Bissell, M., Hall, H., Parry, G. (1982). How does the extracellular matrix direct gene expression? *J. Theor. Biol.*, 99, 31-68.
- [13] Schultz, G., Davidson, J., Kirsner, R., Bornstein, P., Herman, I. (2011) Dynamic reciprocity in the wound microenvironment. *Wound Repair Regen.*, 19, 134-148.
- [14] Sutherland, A., Beck, E., Dennis, S. (2015). Decellularized cartilage may be a chondroinductive material for osteochondral tissue engineering. *PLoS One.*, 10(5), e0121966.
- [15] Taylor, D., Sampaio, L., Ferdous, Z., Gobin, A., Taite, L. (2018) Decellularized matrices in regenerative medicine. *Acta Biomater.*, 74, 74-89.

- [16] Hoch, A., Mittal, V., Mitra, D., Vollmer, N., Zikry, C., Leach, J. (2016) Cell-secreted matrixes perpetuate the bone-forming phenotype of differentiated mesenchymal stem cells. *Biomaterials*, 74, 178-187.
- [17] Agmon, G., Christman, K. (2015). Controlling stem cell behavior with decellularized extracellular matrix scaffolds. *Curr. Opin. Solid State Mater. Sci.*, 20, 193.
- [18] Hellewell, A., Rosini, S., Adams, J. (2017). A rapid, scalable method for the isolation, functional study, and analysis of cell-derived extracellular matrix. *J. Vis. Exp.*, 119, 55051.
- [19] Lin, H., Yang, G., Tan, J., Tuan, R. (2012). Influence of decellularized matrix derived from human mesenchymal stem cells on their proliferation, migration and multi-lineage differentiation potential. *Biomaterials*, 33, 4480-4489.
- [20] Cheng, C., Solorio, L., Alsberg, E. (2014). Decellularized tissue and cell-derived extracellular matrices as scaffolds for orthopaedic tissue engineering. *Biotechnology advances*, 32, 462-484.
- [21] Harvestine, J., Orbay, H., Chen, J., Sahar, D., Leach, K. (2018). Cell-secreted extracellular matrix, independent of cell source, promotes the osteogenic differentiation of human stromal vascular fraction. *J. Mater. Chem. B*, 6, 4104-4115.
- [22] Kusuma, G., Brennecke, S., O'connor, A., Kalionis, B., Heath, D. (2017). Decellularized extracellular matrices produced from immortal cell lines derived from different parts of the placenta support primary mesenchymal stem cell expansion. *Plos One*, 12(2), 0171488.
- [23] Carvalho, M., Silva, J., Cabral, J., Silva, C., Vashishth, D. (2019). Cultured cell-derived extracellular matrices to enhance the osteogenic differentiation and angiogenic properties of human mesenchymal stem/stromal cells. *J. Tissue Eng. Regen. Med.*, 13, 1544-1558.
- [24] Yuan, H., Yang, Z., Bruij, J., Groot, K., Zhang, X. (2001). Material-dependent bone induction by calcium phosphate ceramics: a 2.5-year study in dog. *Biomaterials.*, 22(19), 2617-2623
- [25] Liu, Y., Wang, G., Cai, Y., Ji, H., Zhou, G., Zhao, X., Tnag, R., Zhang, M. (2009). In vitro effects of nanophase hydroxyapatite particles on proliferation and osteogenic differentiation of bone marrow-derived mesenchymal stem cells. *J. Biomed. Mater. Res. A*, 90A(4), 1083-1091.
- [26] He, J., Genetos, D., Leach, J. (2010). Osteogenesis and trophic factor secretion are influenced by the composition of hydroxyapatite/poly (lactide-co-glycolide) composite scaffolds. *Tissue Eng. Part A*, 16(1), 127-137.
- [27] Lee, J., Rim, N., Jung, H., Shin, H. (2010). Control of osteogenic differentiation and mineralization of human mesenchymal stem cells on composite nanofibers containing poly[lactic-co-(glycolic acid)] and hydroxyapatite. *Macromol. Biosci.*, 10(2), 173-182.
- [28] Li, D., Ye, C., Zhu, Y., Qi, Y., Gou, Z., Gao, C. (2012). Fabrication of poly(lactide-co-glycolide) scaffold embedded spatially with hydroxyapatite

- particles on pore walls for bone tissue engineering. *Polym. Adv. Technol.*, 23, 1446-1453.
- [29] Xu, Q., Li, Y., Zhu, Y., Zhao, K., Gu, R., Zhu, Q. (2018). Recombinant human BMP-7 grafted Poly(lactide-co-glycolide)/hydroxyapatite scaffolds via polydopamine for enhanced calvarial repair. *RSC adv.*, 8, 27191-27200.
- [30] Kuljianin, M., Brown, C., Raleigh, M., Lajoie, G., Flynn, L. (2017). Collagenase treatment enhances proteomic coverage of low-abundance proteins in decellularized matrix bioscaffolds. *Biomaterials*, 144, 130-143.
- [31] Kusuma, G., Yang, M., Brennecke, S., O'connor, A., Kalionis, B., Heath, D. (2018). Transferable matrixes produced from decellularized extracellular matrix promote proliferation and osteogenic differentiation of mesenchymal stem cells and facilitate scale-up. *ACS Biomater. Sci. Eng.*, 4, 1760-1769.
- [32] Ding, Y., Floren, M., Tan, W. (2016). Mussel-inspired polydopamine for bio-surface functionalization. *Biosurface and biotribology*, 2, 121-136.

## 국 문 초 록

# 세포외기질이 코팅된 스캐폴드를 이용한 인간 중간엽 줄기세포의 골분화 유도

고 경 원

서울대학교 대학원

협동과정 바이오엔지니어링 전공

우리 몸의 세포외기질인 extracellular matrix(ECM)의 조직특이적인 기계적 및 생화학적 특성을 모방하기 위해 다양한 조직공학적 접근이 이어져왔다. 이중 합성재료를 이용하여 ECM 을 모방한 경우와는 달리 생체조직 및 기관을 탈세포화시켜 만들어낸 decellularized ECM (dECM)이 더 조직특이적 성질을 적합하게 모방할 수 있어 많은 연구진들이 이러한 방안으로 연구를 진행해 왔다. 더 나아가 배양된 세포를 통해 만들어진 cell-derived dECM 이 세포 성장 및 분화를 촉진하는 효율적인 기질로서 사용될 수 있다는 연구도 진행되었다. 세포유래 dECM 을 농축액 상태로 만들어줌과 동시에 ECM 내부 단백질을 유지하게끔 만들어 여러 방향으로 적용될 수 있는 solubilized dECM 이 연구가 되었다. 이렇게 용해된 dECM 은 사용하는 용해 시약에 따라 보유되는 단백질의 구성과 양이 다르므로, 골분화에 효과적인 용해 방법이 필요하다. 그러므로 본 연구는 MC3T3-E1 유래 dECM 을 collagenase (Cg-ECM), pepsin (P-ECM), urea (U-ECM), 그리고 guanidine-HCl (G-ECM)의 여러가지 용해 시약을 사용하여 각각 생산된 solubilized dECM 이 골분화에 미치는 영향을 비교해보았다. 각각의 solubilized dECM 코팅 위에 배양된 세포의 ALP 효소 활성, ARS 광물화 능력 및 osteogenic marker genes 의 발현 정도를 확인하였을

때, G-ECM이 hMSCs의 골 형성 및 분화를 효과적으로 유도하는 결과가 나왔다. 더 나아가, 골 특이적인 scaffold를 만들어주기 위해 PLGA와 hydroxyapatite가 결합됨과 동시에 polydopamine 및 solubilized dECM인 G-ECM이 순차적으로 코팅된 골 분화 특이적 scaffold를 제작하였다. 골분화 효과를 확인해 본 결과, 타 그룹에 비해 G-ECM이 hMSCs의 세포 증식과 골분화를 촉진하였다. 따라서 guanidine-HCl로 용해된 dECM은 골분화를 유도하는 주요 특성을 유지하고, 이를 이용해 만든 스캐폴드는 재생 의학과 조직공학을 위한 새로운 골형성 유도 물질로 사용될 것이다.